VELOCITY DISTRIBUTION CHARACTERISTICS AND PARAMETRIC SENSITIVITY ANALYSIS OF LIQUID NITROGEN JET

Chengzheng Cai[1, 2*] – Gehsheng Li[2] – Zhongwei Huang[2] – Feng Gao[1]

[1]State Key Laboratory for GeoMechanics and Deep Underground Engineering, China University of Mining and Technology, Xuzhou, Jiangsu, 221116, P.R. China
[2]State Key Laboratory of Petroleum Resources and Prospecting, China University of Petroleum, Beijing, 102249, P.R. China

ARTICLE INFO

***Article history*:**
Received: 09.06.2015.
Received in revised form: 01.10.2015.
Accepted: 08.10.2015.

Keywords:
Liquid nitrogen jet
Flow field
Velocity distributions
Numerical simulation

Abstract:

Liquid nitrogen is expected to be used as a jet medium in petroleum engineering because of its cryogenic and non-polluting characteristics. To identify the velocity distribution characteristics of liquid nitrogen jet, a computational fluid dynamics model was built by coupling the equations for nitrogen properties. The velocity and pressure distributions of liquid nitrogen jet were analyzed by comparing them with water jet ones. Meanwhile, the influences of relevant parameters on the centerline velocity distributions of liquid nitrogen jet were researched as well. The simulation results showed that the liquid nitrogen jet not only displayed higher velocity but also presented fewer kinetic energy losses than the water jet during jetting process. The nozzle outlet velocity of liquid nitrogen jet was increased by increasing the nozzle pressure drop, and was slightly influenced by confining pressure and nozzle diameter. In the external space of the nozzle, the attenuation amplitude of centerline velocity was decreased with the growth of nozzle diameter, and was slightly influenced by nozzle pressure drop and confining pressure. This study is expected to provide a theoretical guide for parametric design of liquid nitrogen jet.

1 Introduction

High-pressure water jet technology has played an important role in petroleum engineering, including drilling, sand cleanout, and fracture stimulation [1-4]. However, water jets face several technical and environmental challenges as petroleum engineers increasingly turn their attention to tight formations, such as shale gas, tight gas and coalbed methane. First, large amounts of water are trapped in rocks after drilling, completion, and fracturing because of capillary retention effect, which impedes the flow of gas into wellbore [5, 6]. Second, vast water is consumed during unconventional gas development.

* Corresponding author. Tel.: +86-(0516)-83590619; fax: +86-(0516)-83590619
E-mail address: caichmily@163.com.

For example, over 10 000 m^3 of water is usually required to fracture single horizontal shale well [7]. In addition, water-based work fluids contain a lot of chemical components, which may pollute water resources [8]. Because of the issues mentioned above, substitutes for water-based fluid that are efficient in unconventional gas development and friendly to the environment are increasingly important.

Liquid nitrogen is a colorless and tasteless fluid that is extremely cold at atmosphere pressure (approximately –195.8 °C). It has been successfully used as fracturing fluid in shale and coal formation [9, 10]. Thus, the economic development of unconventional gas with liquid nitrogen jet has proven to be superior not only in preventing formation damage but also in fundamentally solving the problems of water consumption and pollution. Moreover, liquid nitrogen can sharply reduce the temperature around the formation and then induce thermal stress inside rocks, which can initiate the opening of pre-existing cracks and even generate new cracks [11, 12]. Many experimental results have indicated that liquid nitrogen is distinctly advantageous in cracking rocks because of its cryogenic feature [13, 14]. Nonetheless, the characteristics of the jet flow field, especially the distributions of velocity, pressure, and temperature, remain unclear when it comes to the application of liquid nitrogen jet.

To determine the characteristics of liquid nitrogen jet flow field, a computational fluid dynamics (CFD) model was built. Numerical simulation is an effective method for the engineering research and design, which could help realize the visualization of flow field [15, 16]. By coupling the equations to calculate nitrogen properties, velocity and pressure fields of liquid nitrogen jet were simulated. The characteristics of the liquid nitrogen jet flow field were analyzed by comparing them with the ones of water jet flow field. A parametric sensitivity analysis was also performed to identify the influences of nozzle pressure drop, nozzle diameter, confining pressure, and fluid temperature on the distributions of jet centerline velocity. This research could provide theoretical guidance for the application of liquid nitrogen jet.

2 CFD model

2.1 Geometry model and boundaries

A two-dimensional geometry model of the liquid nitrogen jet flow field made up of the internal space of the nozzle and the jet region (external space of the nozzle) was built as shown in Fig. 1. The jet flow field was generated by an axial symmetric nozzle; thus, the half-flow domain is required to be numerically calculated as presented in Fig. 1. During the jetting process, the high-pressure fluid flows through the nozzle and then it is accelerated to a high speed. Consequently, a high velocity jet is generated. In this simulation model, the nozzle inlet was set as pressure inlet boundary and the flow domain outlet was set as pressure outlet boundary. Besides, the jet centerline was set as axial symmetry boundary. The remaining walls were set as non-slip wall boundaries. To eliminate the influences of wall boundaries on jet flow field as much as possible, the external space of the nozzle was set at a relative large value. The distance between the nozzle outlet and the wall boundary orthogonal to the nozzle axis was 600 mm, and the distance between the nozzle outlet and the wall boundary parallel to the nozzle axis was 300 mm.

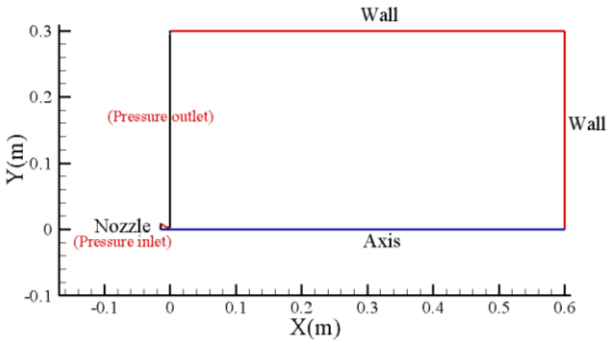

Figure 1. Geometry model of the jet flow field.

To improve calculation accuracy, the grid refinement method (Fig. 2) was applied to the internal flow domain of nozzle, as well as the external flow domain near the nozzle outlet, in which the pressure displayed a large gradient. As depicted in Fig. 2, the structured gird was used to improve the calculation and convergence rates.

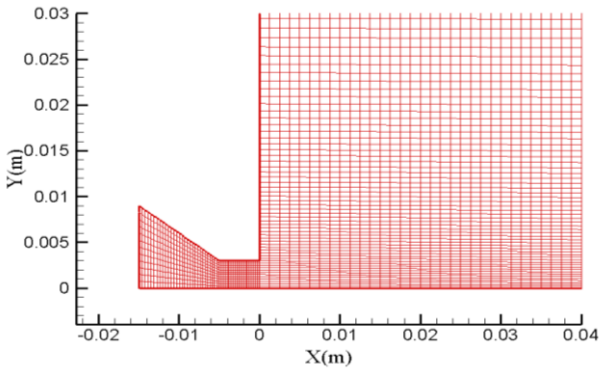

Figure 2. Local grid refinement.

2.2 Mathematical model

The liquid nitrogen jetting process involves heat transfer and compressible fluid. Thus, mass conservation, momentum, and energy conservation equations must be solved. The turbulent flow field would be generated because of the strong shearing effect induced by the high velocity ratio jet [17]. Thus, the standard k-ε model was used to calculate the turbulent flow field. On the compute nodes of the flow domain, the properties of nitrogen were controlled by temperature and pressure. The change in nitrogen properties would influence the flow field in turn. Thus, the properties of nitrogen property equations were also required to be solved.

In our work, the state equation of nitrogen [18], which is explicit in reduced Helmholtz energy, was used to calculate the density and isobaric heat capacity of nitrogen. This equation can be applied to given temperatures ranging from the triple-point temperature to 1000 K and at a maximum pressure of 2200 MPa. It is a highly accurate reference equation for thermodynamic properties of pure nitrogen. When the temperature and pressure are less than 400 K and 1000 MPa, the accuracy ratios of density and isobaric heat capacity are within 1% and 5%, respectively. The Helmholtz energy *(a)* is the function of the density *(ρ)* and temperature *(T)*, namely, $a = a(\rho, T)$. Based on the reduced Helmholtz energy *(α)*, Span et al [16] developed the state equation for nitrogen as shown in Eq. (1). This equation is the function of two independent variables: reduced density *(δ)* and inverse reduced temperature *(τ)*.

$$\alpha(\delta,\tau) = a(\rho,T)/(RT), \quad (1)$$

where, R is the gas constant equal to 0.2968 kJ/(kg·K); $\delta = \rho/\rho_c$, $\tau = T_c/T$; ρ and ρ_c are the density and the critical density, respectively, kg/m^3; T and T_c are the temperature and the critical temperature, K. The critical temperature of nitrogen is 126.492 K, and its critical density is 313.3 kg/m^3.

The reduced Helmholtz energy is expressed in Eq. (2):

$$\alpha(\delta,\tau) = \alpha^o(\delta,\tau) + \alpha^r(\delta,\tau), \quad (2)$$

where, $\alpha^o(\delta, \tau)$ is the ideal - gas component and $\alpha^r(\delta, \tau)$ is the residual part.

The density and isobaric heat capacity of nitrogen are calculated by the following equations:

$$p(\delta,\tau) = \rho RT\left(1 + \delta\left(\frac{\partial\alpha^r}{\partial\delta}\right)_\tau\right), \quad (3)$$

where, p is the pressure, kPa.

$$\frac{C_p(\delta,\tau)}{R} = -\tau^2(\alpha^o_{\tau\tau} + \alpha^r_{\tau\tau}) + \frac{(1 + \delta\alpha^r_\delta - \delta\tau\alpha^r_{\delta\tau})^2}{1 + 2\delta\alpha^r_\delta + \delta^2\alpha^r_{\delta\delta}}, \quad (4)$$

where, C_p is the isobaric heat capacity, kJ/(kg·K).

In addition, viscosity and thermal conductivity were calculated with the model presented by Lemmom and Jacobsen [19]. The viscosity *(η)* is divided into two different terms as in Eq. (5):

$$\eta(\rho,T) = \eta_0(T) + \eta_R(\tau,\delta), \quad (5)$$

where, $\eta_0(T)$ is the viscosity of the dilute gas which depends on temperature (T), Pa·s; $\eta_R(\tau, \delta)$ is the residual part, Pa·s.

The thermal conductivity (λ) is calculated in a similar manner:

$$\lambda(\rho,T) = \lambda_0(T) + \lambda_R(\tau,\delta) + \lambda_c(\tau,\delta), \quad (6)$$

where, $\lambda_0(T)$ is the thermal conductivity of the dilute gas, W/(m·K); $\lambda_R(\tau, \delta)$ is the residual part, W/(m·K); and $\lambda_c(\tau, \delta)$ is the critical enhancement of thermal conductivity, W/(m·K).

2.3 Solver method

As liquid nitrogen jet has high velocity, the gravity can be ignored. To simulate the flow field of liquid

nitrogen jet, the pressure-based solver of commercial CFD software Fluent was adopted [20]. This solver can solve the mass, momentum, and energy equations by coupling the nitrogen properties equations. During the simulation process, the mass and momentum equations were solved first, followed by the energy and turbulence equations. Prior to checking the convergence, the physical properties of nitrogen density, isobaric heat capacity, viscosity, and thermal conductivity were updated according to pressure and temperature on each node [21].

3 Flow field characteristics of submerged liquid nitrogen jet

In order to analyze the characteristics of liquid nitrogen jet, the flow fields of liquid nitrogen jet and water jet have been simulated and then compared with one another. Since water exits in a solid state when the temperature is as low as the liquid nitrogen, jet is unlikely to be formed. In most cases, the thermodynamic parameters of water are usually regarded as the constants. Therefore, the water jet is assumed to have an isothermal flow so that the energy equation is to be ignored. The simulation parameters and thermodynamic parameters of water are set as shown in Table 1.

Table 1. Simulation parameters and thermodynamic parameters of water

Simulation parameters	Value
Diameter of nozzle outlet	6 mm
Diameter of nozzle inlet	18 mm
Confining pressure	30 MPa
Nozzle pressure drop	30 MPa
Temperature of nozzle inlet	100 K
Water density	998.2 kg/m^3
Water viscosity	10.03 × 10^{-4} Pa·s
Water thermal conductivity	0.6 W/(m·K)
Water isobaric heat capacity	4.182 kJ/ (kg·K)

3.1 Model verification using analytical case

The numerical model should be verified by drawing comparisons between analytical solutions or experimental results. As the physical properties of nitrogen changed with pressure and temperature, we selected water as the jet medium to verify the CFD model. In our work, the velocity distributions characteristics of jet flow field was the main research object, so the nozzle outlet velocity was selected as the reference parameter to evaluate the accuracy of numerical solution. In this paper, the numerical model was compared with analytical results which were obtained using Bernoulli's Equation [22]:

$$\frac{p_i}{\rho}+\frac{v_i^2}{2}=\frac{p_o}{\rho}+\frac{v_o^2}{2}, \tag{7}$$

where, p_i and v_i are the pressure and velocity at nozzle inlet, p_o and v_o are the pressure and velocity at nozzle outlet.

According to the mass conservation equation:

$$v_i A_i = v_o A_o, \tag{8}$$

where, A_i and A_o are the section area of nozzle inlet and outlet.

Fig. 3 compares the results from the Bernoulli's Equation and CFD model for different nozzle pressure drops (other calculation parameters were set as presented in Table 1). It indicated that the relative error between analytical and numerical results was less than 5%. Thus, the CFD model can be used to simulate the flow fields of jet.

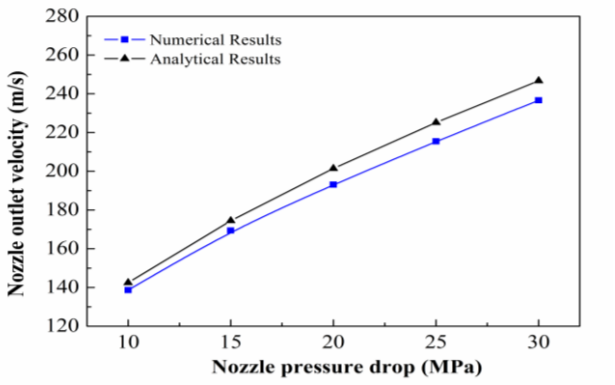

Figure 3. Comparison of numerical and analytical results, nozzle outlet velocity of water jet.

3.2 Velocity distributions

As shown in Fig. 4, when the high pressure flowed through the nozzle, a high velocity jet was induced. During jetting process, the jet velocity decreased significantly with the growth of standoff distance. For the same standoff distance, the liquid nitrogen jet always presented a higher velocity compared

with water jet at the same nozzle pressure drop. In addition, the potential core length of the liquid nitrogen jet was greater than water jet. Thus, liquid nitrogen jet is expected to improve the perforation efficiency and perforation depth because of its higher jet velocity and longer potential core.

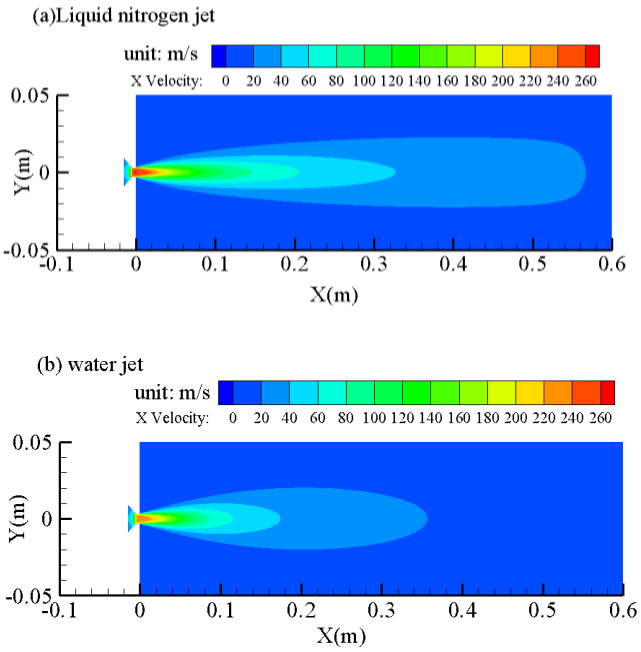

Figure 4. Velocity contours of the liquid nitrogen and water jets in the nearby nozzle.

In order to further analyze the velocity distributions of the liquid nitrogen jet, the centerline velocities of the liquid nitrogen and water jets were compared. As shown in Fig. 5, the maximum centerline velocity of the liquid nitrogen was about 11.74% higher than that of the water jet. In jet region, the centerline velocity was decreasing continuously with the growth of standoff distance due to the friction forces induced by the surrounding fluid. However, the centerline velocity of the liquid nitrogen jet exhibited smaller attenuation amplitude than water jet at the same standoff distance. Take a standoff distance of 200 mm for instance, the centerline velocity of the water jet was 33.95 m/s, which was approximately 14.70% of its maximum velocity. The velocity of liquid nitrogen jet was 61.35 m/s, which was about 23.44% of its maximum value. It suggested that the high pressure liquid nitrogen could be transformed into a higher velocity jet and hence presented fewer kinetic energy losses compared with water jet.

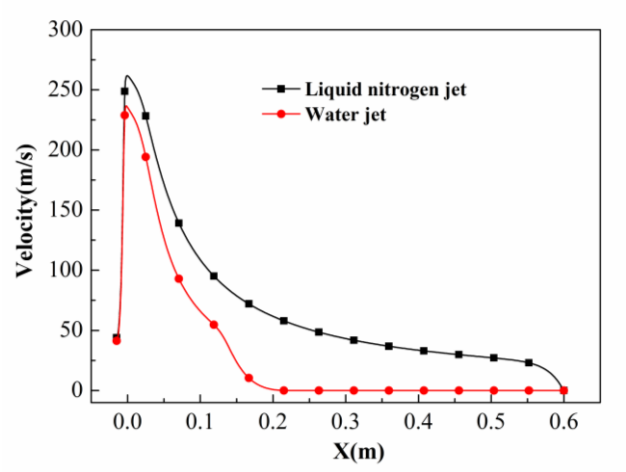

Figure 5. Centerline velocity distribution curves of the jets (Y=0 m).

3.3 Pressure distributions

In order to reveal the pressure distributions of liquid nitrogen jet, the centerline pressures including static, dynamic and total pressures were analyzed. The static pressure is the pressure which is induced by the random motion of fluid molecules, which is positively related to pressure energy. Once the fluid has been in the motion state, dynamic pressure is generated, which determines the degree of fluid kinetic energy. If the gravity is ignored, the sum of the static and dynamic pressures is the total pressure, which is proportional to the mechanical energy of the fluid. As shown in Fig. 6, when the fluid flowed through the nozzle, the static pressure was decreased and the dynamic pressure sharply increased. This indicated that some pressure energy was transformed into kinetic energy. It is also the generation mechanism of high velocity jet. As soon as the jet entered the external space of the nozzle, the dynamic and total pressures were considerably decreased, whereas the static pressure was hardly changed. This suggested that the attenuation of jet velocity was mainly caused by kinetic energy loss. As depicted in Fig. 6, the total and dynamic pressures of the liquid nitrogen jet were always greater than those of water jet along the jet centerline, indicating fewer kinetic energy losses for liquid nitrogen jet than water jet. For example, the total and dynamic pressures of liquid nitrogen jet were 32.96 MPa and 2.95 MPa, respectively at the standoff distance of 130 mm, while those of the water jet were 31.06 MPa and 0.95 MPa.

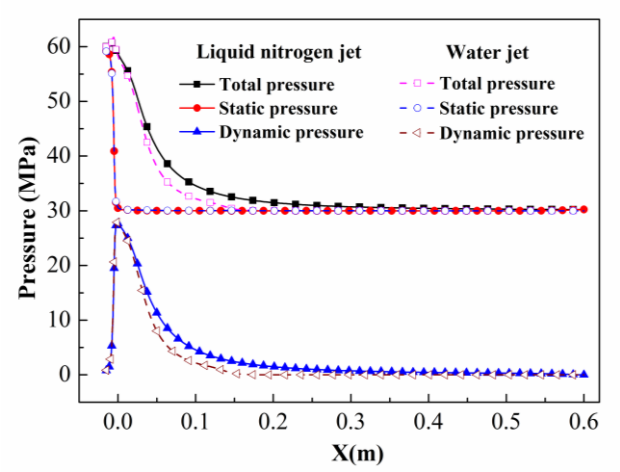

Figure 6. Distributions of the centerline pressures of the jets (Y=0 m).

3.4 Distributions of density and viscosity

To explore the reason why liquid nitrogen presented higher velocity and fewer kinetic energy losses, the liquid nitrogen density and viscosity distributions along the jet centerline were analyzed. As shown in Fig. 7, during liquid nitrogen jetting process, the density of liquid nitrogen ranged from 768.86 to 841.72 kg/m^3, which was less than that of water (998.2 kg/m^3). That was the reason why liquid nitrogen jet displayed a higher velocity than water jet at the same nozzle pressure drop. In addition, the viscosity of liquid nitrogen was about 10% of water.

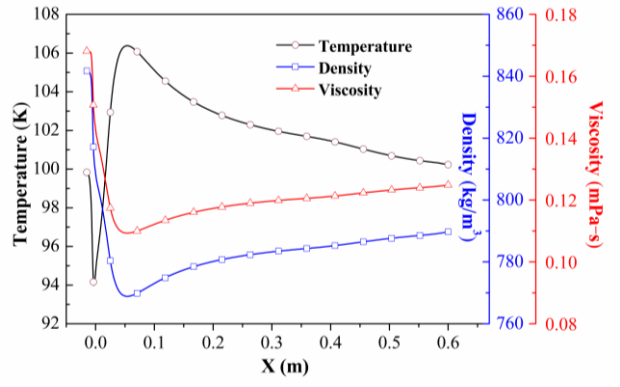

Figure 7. Centerline temperature, density, and viscosity distributions of liquid nitrogen jet (Y=0 m).

So, the friction force to which liquid nitrogen jet had to be subjected was less than that of the water jet. As a result, the jet velocity, kinetic pressure and total pressure of liquid nitrogen were less attenuated than those of water jet.

4 Parametric sensitivity analysis on centerline velocity distribution of liquid nitrogen jet

As presented in Fig. 4, the jet velocity near the nozzle was homogenous. The jet drew the fluid around it and carried it away because of its viscosity. As a result, jet flow widened and the jet velocity decreased gradually. According to jet theory, the centerline velocity of jet is an important parameter in evaluating its operational capability [23]. Thus, the distributions and attenuation characteristics of jet centerline velocity should be analyzed. In order to research the jet centerline velocity distribution characteristics of liquid nitrogen jet, the centerline velocity distributions under different conditions were simulated and a parametric sensitivity analysis was performed. In our work, the velocity at the nozzle outlet and the dimensionless centerline velocity, which was defined as the ratio of centerline velocity (v_c) to nozzle outlet velocity (v_o), were selected as the characteristic parameters.

4.1 Nozzle pressure drop

For liquid nitrogen jet, the nozzle pressure drop is an important parameter that determines the value of jet kinetic energy. As shown in Fig. 8, the nozzle outlet velocity of liquid nitrogen jet was increased almost linearly with the growth of nozzle pressure drop. For instance, this velocity was increased by 73.3% (from 151.06 m/s to 261.72 m/s) with an increase in the nozzle pressure drop from 10 MPa to 30 MPa. This was because with the growth of nozzle pressure drop, the kinetic energy was increased accordingly. Consequently, jet velocity increased at the nozzle outlet.

Fig. 9 depicts the distribution curves of the dimensionless centerline velocity of liquid nitrogen jet at different nozzle pressure drops. As shown in Fig.9, the dimensionless centerline velocity was slightly increased with the growth of the nozzle pressure drop. When we took a standoff distance of 60 mm, for example, the dimensionless centerline velocity was increased from 0.46 to 0.58 as the nozzle pressure drop was increased from 10 MPa to 30 MPa. This result was attributed to the fact that the viscosity of liquid nitrogen changed slightly in

the jet flow region, as indicated in Fig. 7. Thus, the friction forces of the surrounding fluid remained almost constant along the centerline. The nozzle pressure drop mainly determined nozzle outlet velocity, and its influence on centerline velocity distributions was limited.

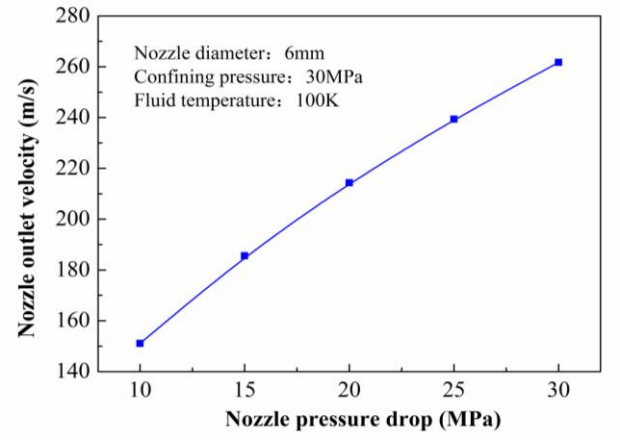

Figure 8. Effect of nozzle pressure drop on nozzle outlet velocity.

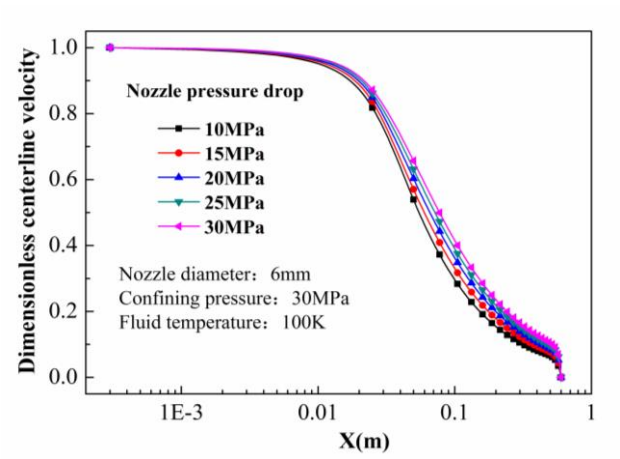

Figure 9. Distributions of the dimensionless centerline velocity of the liquid nitrogen. jet given different nozzle pressures (Y=0 m).

4.2 Nozzle diameter

Fig. 10 exhibits the relationship between nozzle outlet velocity of liquid nitrogen jet and nozzle diameter. As shown in this figure, the nozzle diameter hardly affected the outlet velocity of liquid nitrogen jet. For example, the nozzle outlet velocity was increased only by about 3.57% even though the nozzle diameter was increased from 4 mm to 8 mm with an increase of 100%. This was because that the growth of nozzle diameter mainly widened the jet flow section area, but exhibited little effect on the kinetic energy per unit area of jet region.

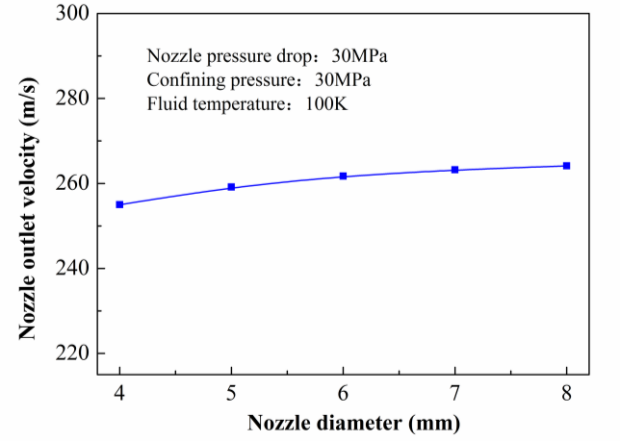

Figure 10. Effect of nozzle diameter on nozzle outlet velocity.

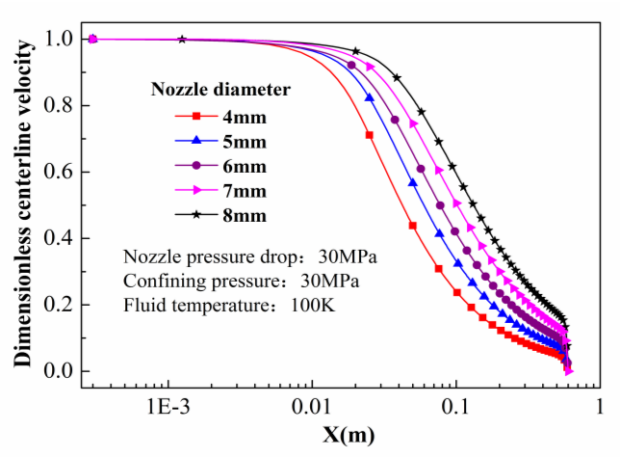

Figure 11. Distributions of the dimensionless centerline velocity of the liquid nitrogen jet given different nozzle diameters (Y=0).

As shown in Fig. 11, the length of potential core and the dimensionless centerline velocity of the liquid nitrogen jet was considerably increased with an increase in nozzle diameter. At the standoff distance of 30 mm, the dimensionless centerline velocities of nozzles with diameters of 4, 5, 6, 7, and 8 mm were 0.64, 0.76, 0.83, 0.88, and 0.93, respectively. This indicated that the attenuation

amplitude of centerline velocity was decreased with the growth of nozzle diameter. It was due to the liquid nitrogen jet which was generated with a larger nozzle, which in turn displayed a wider jet flow region at the same nozzle pressure drop. Therefore, the jet velocity in the potential core had greater total kinetic energy and the fluid near the centerline was less influenced by the surrounding fluid. In this case, the attenuation amplitude of centerline velocity of liquid nitrogen jet was decreased with an increase in nozzle diameter.

4.3 Confining pressure

The effect of confining pressure on centerline velocity distributions of liquid nitrogen jet was also studied. As shown in Fig. 12. The outlet velocity of liquid nitrogen jet was slightly decreased with an increase in confining pressure. When the confining pressure was 10 MPa, the nozzle outlet velocity was 268.21 m/s. This velocity decreased by 2.42% when the confining pressure increased from 10 MPa to 30 MPa. This indicated that the confining pressure was slightly influenced with the outlet velocity of liquid nitrogen jet. It was because the confining pressure affected only the pressure level of the whole jet flow field and hardly affected the kinetic energy of the fluid. (Consequently, only the pressure level of the whole jet flow was largely affected by the confining pressure but not the kinetic energy of the fluid.) Thus, the liquid nitrogen jet velocity at nozzle outlet changed little with the variation of confining pressure.

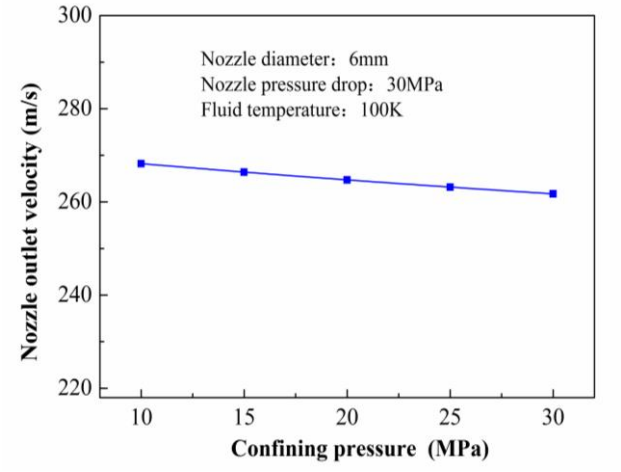

Figure 12. Effect of confining pressure on nozzle outlet velocity.

As presented in Fig. 13, the dimensionless centerline velocity exhibited also hardly any changes with variations of confining pressure. Given a standoff distance of 120 mm for example, the dimensionless centerline velocity was merely decreased from 0.42 to 0.36 when the confining pressure was increased from 10 MPa to 30 MPa. This indicated that the confining pressure exerted quite a limited influence on the attenuation amplitude of centerline velocity. Thus, nozzle outlet velocity and effective operation distance would not be reduced with the growth of confining pressure. This result suggested that the liquid nitrogen jet could maintain an excellent jetting effect even under high confining pressure condition.

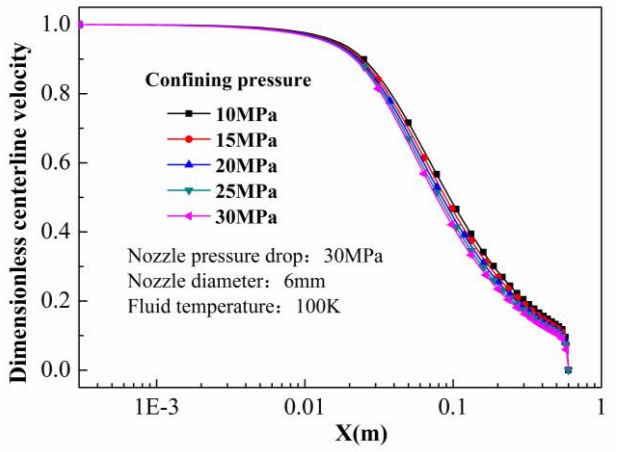

Figure 13. Distributions of the dimensionless centerline velocity of the liquid nitrogen jet given different confining pressures (Y=0 m).

5 Conclusions

The flow field characteristics of liquid nitrogen jet were studied with the CFD method and also the centerline velocity distributions analyzed. The main conclusions can be summarized as follows:

(1) The velocity of liquid nitrogen jet was higher than that of water jet at the same nozzle pressure drop due to its lower density. Thus, liquid nitrogen jet is expected to present more excellent performances on rock perforation than those in water jet.

(2) In the external space of nozzle, the attenuation amplitude of liquid nitrogen jet velocity was smaller compared to water jet at the same standoff distance. So, liquid nitrogen jet had a longer potential core

compared to water jet, which was beneficial to improve the perforation depth.
(3) The nozzle outlet velocity of liquid nitrogen jet was obviously increased by increasing nozzle pressure drop but was also hardly influenced by the confining pressure and nozzle diameter.
(4) The attenuation amplitude of velocity of liquid nitrogen jet was apparently decreased with an increase in nozzle diameter. However, it was not significantly influenced by nozzle pressure drop and confining pressure.

Acknowledgments

This work was financially supported by the National Natural Science Foundation of China (51323004 & 51374220) and the Foundation of State Key Laboratory of Petroleum Resources and Prospecting (PRP/open - 1507).

References

[1] Li, G., Huang, Z., Tian, S., Shen, Z.: *Research and application of water jet technology in well completion and stimulation in China*, Petrol. Sci., 7(2010), 2, 239-244.
[2] Bi, G., Li, G., Ma, D., Shen, Z., Huang, Z., Li, J., Yang, R.: *Mathematical modeling and experiment on propulsion of the multijet bit*, At. Sprays., 24(2014), 9, 761-778.
[3] Qu, H., Li, G., Huang, Z., Xia, Q.: *Research on hydraulic parameters and field tests of horizontal wells sand-flushing with rotating jet*s, Energy Source Part A, 35(2013), 16, 1566-1573.
[4] Tian, S., Li, G., Huang, Z., Niu, J., Xia, Q.: *Investigation and application for multistage hydrajet-fracturing with coiled tubing*, Petroleum Science and Technology, 27(2009), 13, 1494-1502.
[5] Bahrami, H., Rezaee, M.R., Nazhat, D.H., Ostojic, J., Clennell, M.B., Jamili, A.: *Effect of water blocking damage on flow efficiency and productivity in tight gas reservoirs*, SPE Production and Operations Symposium, Oklahoma City, Oklahoma, USA, 2011.
[6] Bennion, D.B., Thomas, F.B., Bietz, R.F.: *Low permeability gas reservoirs: Problems, opportunities and solutions for drilling, completion, stimulation and production*, SPE Gas Technology Conference, Calgary, Alberta, Canada, 1996.
[7] Bryant, J.E., Haggstrom, J.: *An environmental solution to help reduce freshwater demands and minimize chemical use*, SPE/EAEG European Unconventional Resources Conference and Exhibition, Vienna, Austria, 2012.
[8] Holtsclaw, J., Loveless, D.M., Saini, R.K., Fleming, J.: *Environmentally focused crosslinked-gel system results in high retained proppant-pack conductivity*, SPE Annual Technical Conference and Exhibition, Denver, Colorado, USA, 2011.
[9] Mcdaniel, B.W., Grundmann, S.R., Kendrick, W.D.: *Field applications of cryogenic nitrogen as a hydraulic fracturing fluid*, SPE Annual Technical Conference and Exhibition, San Antonio, Texas, USA, 1997.
[10] Grundmann, S.R., Rodvelt, G.D., Dials, G.A., Allen, R.E.: *Cryogenic nitrogen as a hydraulic fracturing fluid in the devonian shale*, SPE Eastern Regional Meeting, Pittsburgh, Pennsylvania, 1998.
[11] Kim, K.M., Kemeny, J.: *Effect of thermal shock and rapid unloading on mechanical rock properties*, 43rd US rock mechanics symposium and 4th U.S. - Canada rock mechanics symposium, Asheville, North Carolina, USA, 2009.
[12] Tran, D., Settari, A., Nghiem, L.: *Initiation and propagation of secondary cracks in thermo-poroelastic media*, 46th US Rock Mechanics /Geomechanics Symposium, Chicago, Illinois, USA, 2012.
[13] Ren, S., Fan, Z., Zhang, L., Yang, Y., Luo, J., Che, H.: *Mechanisms and experimental study of thermal-shock effect on coal-rock using liquid nitrogen*, Chinese Journal Rock Mechanical Engineering, 32(2013), S2, 3790-3794 [in Chinese].
[14] Cai, C., Li, G., Huang, Z., Shen, Z., Tian, S.: *Rock pore structure damage due to freeze during liquid nitrogen fracturing*, Arabian Journal for Science and Engineering, 39(2014), 12, 9249-9287.
[15] Guofa, M., Chuangyun, L., Zeng, G.; *Application of numerical simulation on cast steel toothed plate*. Engineering Review, 34(2014), 1, 1-6.

[16] Čarija, Z., Marušić, E., Novak, Z., Fućak, S.; *Numerical analysis of aerodynamic characteristics of a bumped leading edge turbine blade*. Engineering Review, 34(2014), 2, 93-101.
[17] Sheng, M.; Li, G.; Huang, Z.; Tian, S., Qu, H.; Wu. C.: *Numerical simulation of pressure boosting effect in jet hole during hydrajet fracturing*. Drilling & Production Technology, 34(2011), 2, 42-45 [in Chinese].
[18] Span, P., Lemmon, E.W., Jacobsen, R.T., Wagner, W., Yokozeki, A.: *A reference equation of state for the thermodynamic properties of nitrogen for temperatures from 63.151 to 1000 K and pressures to 2200 MPa*, Journal of Physical and Chemical Reference Data., 29(2000), 6, 1361-1433.
[19] Lemmon, E.W., Jacobsen, R.T.: *Viscosity and thermal conductivity equations for nitrogen, oxygen, argon, and air*, International Journal of Thermophysics., 25(2004), 1, 21-69.
[20] Wang, F.: *Computational fluid dynamics analysis*, Tsinghua University Press, Beijing, 2004 [in Chinese].
[21] Guardo, A., Coussirat, M., Recasens, F., Larrayoz, M. A., Escaler, X.: *CFD study on particleto-fluid heat transfer in fixed bed reactors: convective heat transfer at low and high pressure*, Chemical Engineering Science., 61(2006), 13, 4341–4353.
[22] Munson, B.R., Young, D.F., Okiishi, T.H.: *Fundamentals of fluid mechanics*, John Wiley & Sons Inc., New Jersey, 1990
[23] Li, G., Shen, Z.: *Theory and application of self- resonating cavitating water jet*, China University of Petroleum Press, Dongying, 2008 [in Chinese].